Environmental Science & Technology

Article

pubs.acs.org/est

Mobile Laboratory Observations of Methane Emissions in the Barnett Shale Region

Tara I. Yacovitch,*[,†] Scott C. Herndon,[†] Gabrielle Pétron,[‡,§] Jonathan Kofler,[‡,§] David Lyon,[∥] Mark S. Zahniser,[†] and Charles E. Kolb[†]

[†]Aerodyne Research Inc., Billerica, Massachusetts 01821, United States

[‡]Cooperative Institute for Research in Environmental Sciences, University of Colorado Boulder, Boulder, Colorado 80309, United States

[§]NOAA Earth System Research Laboratory, Boulder, Colorado 80309, United States

[∥]Environmental Defense Fund, 301 Congress Ave Suite 1300, Austin, Texas 78701, United States

Supporting Information

ABSTRACT: Results of mobile ground-based atmospheric measurements conducted during the Barnett Shale Coordinated Campaign in spring and fall of 2013 are presented. Methane and ethane are continuously measured downwind of facilities such as natural gas processing plants, compressor stations, and production well pads. Gaussian dispersion simulations of these methane plumes, using an iterative forward plume dispersion algorithm, are used to estimate both the source location and the emission magnitude. The distribution of emitters is peaked in the 0−5 kg/h range, with a significant tail. The ethane/methane molar enhancement ratio for this same distribution is investigated, showing a peak at ∼1.5% and a broad distribution between ∼4% and ∼17%. The regional distributions of source emissions and ethane/methane enhancement ratios are examined: the largest methane emissions appear between Fort Worth and Dallas, while the highest ethane/methane enhancement ratios occur for plumes observed in the northwestern potion of the region. Individual facilities, focusing on large emitters, are further analyzed by constraining the source location.

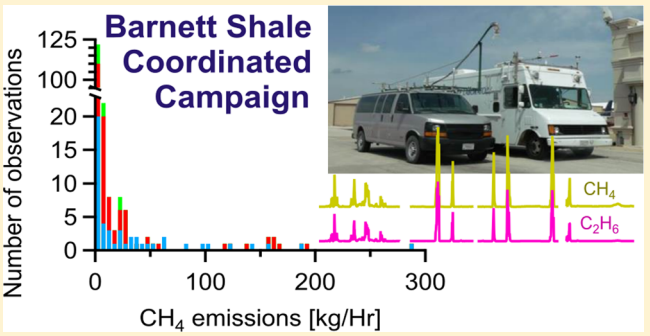

INTRODUCTION

The Barnett Shale play in north central Texas was the first major shale gas basin in the United States to feature the combination of horizontal drilling and hydraulic fracturing known as unconventional gas exploration and production. Oil and natural gas production requires numerous pieces of equipment that are potential emission sources, including well heads; liquid storage tanks for produced water, condensate or crude oil; natural gas compressor stations, processing plants and gathering stations; gas flares; gathering and transmission pipelines; and more. The Barnett region is also home to the large metropolitan area of Dallas/Fort-Worth which includes urban sources of methane such as landfills and wastewater treatment plants. The Barnett Shale Coordinated Campaign is a 2013 Environmental Defense Fund (EDF) study aimed at quantifying the methane emissions from shale gas operations in the Barnett region. This study involved multiple research teams and several ground-based and aircraft-based measurement platforms.[1]

In this paper, we describe the results of mobile measurements conducted in the Aerodyne Mobile Laboratory (AML) and the NOAA Global Monitoring Division (GMD) instrumented van. Methane and ethane measurements are conducted during on-road drives, mapping background concentrations and intercepts of methane emission plumes. Gaussian dispersion calculations are used to estimate methane emissions associated with observed plumes of enhanced methane. The regional distribution of estimated emission magnitudes is examined and compared with the regional distribution of observed ethane/methane enhancement ratios. Emissions from selected individual facilities, including gas processing plants, compressor stations and well pads, are simulated with enhanced detail by constraining source locations.

EXPERIMENTAL METHODS

During the spring and fall of 2013, the Aerodyne Mobile Laboratory[2] (AML) and the NOAA GMD van[3] drove through the Barnett shale region near Dallas Fort-Worth. All measurements were made on public roads and without site access. Two sampling strategies were employed: deliberate transects down-

Received: December 31, 2014
Revised: February 20, 2015
Accepted: February 23, 2015
Published: March 9, 2015

DOI: 10.1021/es506352j
Environ. Sci. Technol. 2015, 49, 7889−7895

wind of large facilities as characterized by their 2012 EPA Greenhouse Gas Reporting Program[4] (GHGRP) emissions and transects through the region, acquiring plumes from any point source upwind of the drive path.

Mobile Laboratories. The Aerodyne Mobile Laboratory (AML) is an instrumented step van with gas-phase and particle-phase measurement capabilities.[2,5] For the data acquired and described within, no particulate measurements were conducted.

The gas phase inlet extends out of the front of the passenger-side cab (~2.75 m above ground). An overblow port near the inlet tip allows for timed deliveries of clean air for instrument zero checks. Calibrations are also done periodically through this port. A length of $^1/_2$ in. Teflon tubing runs along the inside of the AML into a pressure controller. Three Aerodyne Tunable IR Laser Direct Absorption Spectroscopy (TILDAS) instruments are operated in series at subambient pressures behind this pressure controller: a QCL-Dual chassis[6] is equipped to measure methane, water, acetylene, and sulfur dioxide; a QCL-mini measures ethane; a second QCL-mini measures nitrous oxide, carbon monoxide and water vapor.[7] The first two of these instruments use the overblow periods to perform spectroscopic background subtraction for enhanced accuracy. A scroll pump provides ~12 L/min of flow through the inlet and past these TILDAS instruments. Several more instruments are operated in parallel drawing from the near-atmospheric pressure portion of the inlet, prior to the pressure controller: a LiCor CO_2 analyzer; and a Thermo Fischer NO_x detector. A diaphragm pump provides a dump flow, ensuring that no portion of the common inlet and overblow tubing is stagnant.

Geographic and meteorological parameters are also measured during the experiment. Redundant position information is obtained via several on-board GPS sensors including a Garmin hand-held device, and a Hemisphere V100 GPS Compass. A sonic anemometer (Airmar 200WX) mounted to the AML's mast provides true wind measurement and another redundant GPS measurement. A rotary vane anemometer provides a secondary wind measurement (Vaisala WM30). The wind measurements are corrected for the effect of mobile lab motion using the GPS position and bearing information from the GPS compass measurement.

Data from all instruments are logged and saved using the DataLogger program written at Aerodyne Research, Inc. (ARI). The data exchange via file transfer (DEFT) protocol allows the main data display computer to load data from all instruments semicontinuously. Note-taking and annotation capabilities are integrated into the data display, allowing the operator to identify and record specific events as they occur.

The NOAA GMD instrumented van[3] is equipped with a methane analyzer measuring CH_4, CO_2 and H_2O (Picarro CRDS).[8] Flasks sampling can be triggered to collect air during interesting events from an inlet colocated near the inlet of the continuous analyzer toward the front of the van. A GPS monitor provides position information. For one overnight drive in April of 2013, an Aerodyne Ethane-mini instrument[7] was installed in the NOAA GMD instrumented van. The Ethane-mini instrument, integrated pressure controller, chiller and a small Agilent IDP 3 dry scroll vacuum pump were used. The instrument used a separate inlet tube terminating at the tip of the van's lofted inlet. The ethane instrument was run without spectroscopic backgrounding; comparisons of data in the days prior to this outing showed negligible differences between the backgrounded and unbackgrounded retrieved mixing ratios (<0.5 ppb).

Meteorological data from several weather stations were obtained via Weather Underground[9] and used to supplement the onboard wind measurement. These data also provide information on cloud coverage for use in the Gaussian dispersion simulations described below.

Gaussian Dispersion Calculations. The dispersion modeling described below is based on the standard Gaussian dispersion equations and procedures.[10] Equation 1 relates the measured concentration of emissions (C) at a position x meters downwind, y meters off-axis, and z_r meters above ground. The source emission rate (Q), the horizontal wind velocity (u) and the height above ground of the plume centerline (H_e) are required, along with terms for vertical (σ_z) and horizontal (σ_y) dispersion. These dispersion terms are taken from a lookup table based on a chosen Pasquill stability class and are a function of x, the downwind distance.

$$C = \frac{Q}{u\sigma_z\sigma_y 2\pi} e^{-y^2/2\sigma_y^2}\left(e^{-(z_r-H_e)^2/2\sigma_z^2} + e^{-(z_r+H_e)^2/2\sigma_z^2}\right) \quad (1)$$

The Pasquill stability classes define the chosen σ_y σ_z and describe the extent of spread that a simulated plume undergoes as it is transported downwind. The stability class for these results was chosen based on measured or archived meteorological data using the STAR method,[10,11] further described in the SI. This procedure determines the stability class based on measured wind speed, solar elevation, cloud coverage, cloud ceiling height and whether it is day or night. Six stability classes are allowed, A through D in the day and E and F at night. These classes span conditions ranging from the least stable (most turbulent) and most stable (least turbulent), respectively.

The experimental data used in these simulations consist of periods of data, typically 1−5 min long, taken in motion, and showing the methane mixing ratio rise and then fall above a nominal background value. This technique transects the entire spatial extent of a plume and differs from other methods using stationary sampling combined with measurements of wind fluctuations to build a Gaussian plume.[12,13]

Several oil and gas facilities with large reported methane emissions were visited during this campaign. Emissions from these facilities were investigated using the simplest application of the Gaussian dispersion calculation: *fixed release location*. This analysis requires choosing a single point source location based on the known facility address, wind direction and inspection of satellite map imagery. The stability class for the time period of measurement is determined as above. A 1 g/sec methane emission is simulated and projected onto the downwind transect. The emission magnitude is estimated by determining a scaling ratio between the measured plume and the simulated plume; the slope of the linear fit of measured vs simulated mixing ratios provides this ratio.

For certain emitters, a single point source simulation cannot fully reproduce the observed methane enhancements during downwind transects. One such situation arises when a close transect is done downwind of a large site with multiple distinct emission sources, such as a processing plant with multiple compressor houses, flares, valve or piping leaks, etc. Each plume may be more or less distinct in the resulting transect. In these cases, a *multisource fixed release location* method is used. Numerous emission sources are chosen based on inspection of a satellite map. Simulations for these facilities are performed by manually varying the magnitude of each point source and

DOI: 10.1021/es506352j
Environ. Sci. Technol. 2015, 49, 7889−7895

Table 1. Simulated Methane Emission Results for Individual Facilities[a]

facility name	facility type	facility latitude	facility longitude	sim. emis (kg/h)	95% CI (kg/h)	C_2H_6/CH_4 · 100%	no. plumes
processing plant, Bridgeport TX	processing	33.19582	−97.80396	193	[64, 645]	1.1−16%	6
processing plant, Eagle Mountain TX	processing	32.90927	−97.47289	169	[56, 564]	1.8%	2
processing plant, Pecan Acres TX	processing	32.96841	−97.48126	163	[54, 544]	2.5%	2
processing plant, Rhome TX	processing	33.05244	−97.41140	162	[54, 541]	3.3%	1
gathering station, Denton TX	compressor	33.09500	−97.26400	1360	[454, 4542]	1.1−1.9%	1
gathering station, Cleburne TX	compressor	32.42910	−97.17770	406	[136, 1356]	1.4%	1
compressor station, Eagle Mountain TX[b]	compressor	32.91862	−97.40316	51	[17, 170]	1.4%	4
compressor station, Justin TX[b]	compressor	33.12543	−97.33899	23	[8, 77]	2.8−5.3%	3
compressor station, Rhome TX[b]	compressor	33.03353	−97.34767	23	[8, 77]	2.5%	1
compressor station, Denton TX	compressor	33.19783	−97.06672	4	[1, 13]	1.8%	2
well pad, Boyd TX	well pad	33.06347	−97.56362	287	[96, 959]	11%	1
well pad, Justin TX	well pad	33.10159	−97.28684	189	[63, 631]	2.8%	1
well pad, DISH TX[b]	well pad	33.14858	−97.29874	155	[52, 518]	6.8%	5
well pad, Fort Worth TX	well pad	32.90252	−97.46308	136	[45, 454]	1.2%	4
well pad, Haslet TX	well pad	33.03037	−97.37359	124	[41, 414]	4.5%	1
well pad, Newark TX	well pad	33.00862	−97.50763	62	[21, 207]	3.3%	1
well pad, Krum TX	well pad	33.26423	−97.27217	6	[2, 20]	16%	1
roadside piping, Eagle Mountain TX	piping	32.90986	−97.46696	2.5	[1, 8]	3.10%	4

[a]Simulated emissions in kg/h are reported along with the 95% confidence intervals (CI) as calculated from the method error (factor of 0.334 and 3.334). The ethane/methane enhancement ratio for these facilities is also shown (C_2H_6/CH_4 · 100%). [b]Facility location is certain. See Text.

summing their simulated plumes in order to best reproduce the spatial structure of the measured plume

Iterative Forward Dispersion Calculations. The methods described above assume knowledge of a source's location. The majority of the data acquired for this study consists of "accidental" plumes acquired in between measurements of large facilities and during long drives across the study region. The totality of the experimental data was manually divided into individual "plumes" based on the ethane/methane enhancement ratio. For these plumes, an automated method to guess source location was developed.

The *iterative forward dispersion* method begins by choosing an array of potential source locations upwind of the measured plume. Each candidate source location is passed through the standard Gaussian simulation procedure defined above, and the chi-square value between the optimally scaled plume simulation and the measurement is calculated. The simulation with the smallest chi-square best matches the shape of the experimental data, and is used to determine the "best" source location. Subsequent automated and manual data set filtering (see SI) reduces the number of valid simulations. This method was applied to the entirety of the data set, approximately 500 separate segments. Of these, 223 plumes passed the automated and manual quality tests. This method and data treatment is described in detail in the SI.

Method Validation and Error Estimates. There are several assumptions involved in Gaussian plume simulations and the Pasquill stability classes,[10,14−17] and thus several possible sources of systematic error in these emission flux determinations. First, no fluctuations are allowed in either the emission flux, or the average wind direction in the time it takes a plume to be emitted and reach the measurement location (∼2−20 min). Second, the stability class determination is assumed to be valid for the data in question. Third, the time scale of the measurement transect is assumed to be at the same time scale as that which the stability class parameters were developed (∼3−60 min).[16] Further assumptions are included in this particular study in order to allow for the automated processing of all data. It is assumed that emission and receptor height is fixed to 0 m above ground, meaning that close transects downwind of a tall emission stack (or buoyant plume) will not be properly simulated (and may in fact not be acquired by the measurements).

The assumptions listed above can all have major effects on the results of a simulation, and thus in the determination of an emission magnitude and location based on experimental data. The question of time scales and the applicability of the concept of a stability class to transect data are of particular interest. Beychok describes the effects of different mixing ratio averaging time scales in the measured emissions,[10] and Fritz et al. describe the scaling of wind measurements and associated stability classes with averaging time.[14] These questions warrant further investigation using high-frequency meteorological instruments and additional metered trace gas releases or parallel emissions determinations using Gaussian dispersion on the one hand and tracer release[18,19] on the other, and are beyond the scope of this publication.

A 5-day data set of metered tracer release data was used to test the Gaussian dispersion flux quantification method. This data set included 141 transected plumes, each containing 2−5 different chemical tracers (see SI). The 95% confidence intervals (CI) for the Gaussian dispersion method flux quantification are nonsymmetrical and expressed as a fraction of the simulated emission; for a simulated emission x, the 95% CI are $[0.334{\cdot}x, 3.34{\cdot}x]$ (see SI). These error bounds are within the range of model sensitivity analyses performed by others.[10,14−17] They can also be compared to the EPA Other Test Method 33A recently described by Brantley et al.:[13] a Gaussian dispersion approach using stationary measurements and a custom set of atmospheric stability classes. The EPA test method was also verified using staged release data to determine errors of ±60%. These are not formal 95% confidence bounds since all data points are included, but translate roughly to errors of $[0.40{\cdot}x, 1.6{\cdot}x]$ in the same notation as above.

DOI: 10.1021/es506352j
Environ. Sci. Technol. 2015, 49, 7889−7895

RESULTS AND DISCUSSION

Regional Methane Emissions. Gaussian simulation of 224 measured methane plumes at different locations throughout the Barnett Shale region leads to a broad range of methane emission estimates, 0.006−571 kg/h. Since duplicate measurements of sources are present in the *iterative forward dispersion* results, a clustering of points was performed, combining sources simulated within 500 m of each other if they had ethane/methane molar enhancement ratios within 0.5%, yielding 188 data points. When available, data from those sources whose positions were fixed (Table 1 and following section) replace the *iterative forward dispersion* results. Data from Figure 1A show

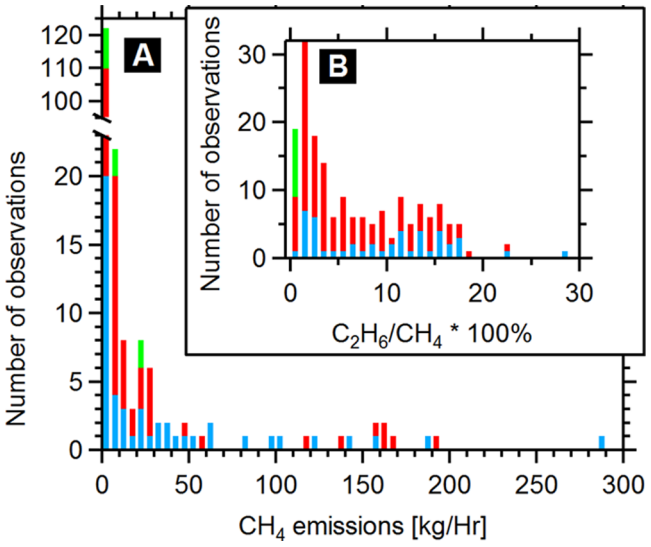

Figure 1. Distribution of 188 methane emissions estimates (Panel A) and ethane/methane molar enhancement ratios (Panel B). Oil and gas sources (172 sources) are shown as red bars, with the contribution of well pads (49 sources) highlighted in blue. Biogenic emitters (16 sources) are shown as green bars atop the red oil and gas distribution.

the resulting distribution of methane emitters, excluding the two largest methane emitters sampled (406 kg/h and 1360 kg/h). Figure 1B shows the distribution of ethane/methane ratios for this same population; three high ratios are not shown (80%, 93%, and 100%). Oil and gas sources are drawn in red, with the contribution of well pad sources highlighted in blue. The green bar in this histogram corresponds to sources identified as purely biogenic. These include sources such as cattle rumination and stagnant water, where methane emissions are observed with no concomitant enhancement in ethane.

The distribution of methane emitters (Figure 1A) is peaked at low emission rates, with 81% of simulated plumes estimated at 10 kg/h or less. The distribution also has a substantial tail with 7.5% of emitters contributing to 60% of the total simulated emissions. There is a slight enhancement in the number of sources found in the 70−100 kg/h range, but data is sparse in the distribution tail. This enhancement may be a result of sampling bias; the geographic region visited and sample of sources measured was not statistically random, since several natural gas facilities with large inventory emissions were visited deliberately. Emissions estimates from well pads (Figure 1A, blue bars) identified via satellite maps make up a substantial number of the observed oil and gas sources and show a similar distribution shape as the full oil and gas emissions distribution (see SI).

The ethane content of methane emissions can reveal information about the emission source. The measured ethane/methane enhancement ratios for the simulated methane sources in this study vary greatly, ranging from 0% (no observed ethane) all the way to 100% (molar ethane enhancement equals the molar methane enhancement). In fact, in one case not included in the methane results here, a plume of pure ethane was measured (see SI). The frequency of sources with a given ethane/methane ratio is shown in the inset in Figure 1. This distribution shows a clear peak at ∼1.5%, with a broad continuum between ∼4 and ∼17%. These ethane/methane ratios can be compared to those found by analyzing flight data from the Barnett Shale Coordinated Campaign,[20] and discussed in detail in Smith et al.[21] In that analysis, one microbial and two fossil fuel source ratios are observed at 0.0%, 1.8%, and 9.6%, respectively, and used in partitioning the total basin methane flux between biogenic and thermogenic sources. The ground data supports this analysis, with discrepancies attributed mainly to differences in the regions sampled.

The regional distribution of the simulated sources was investigated using a 2-dimensional binning method. Each bin covers 10 km^2 of the area driven. The average emission value for all sources originating from each bin is computed, and plotted in Figure 2 below. The region of highest average

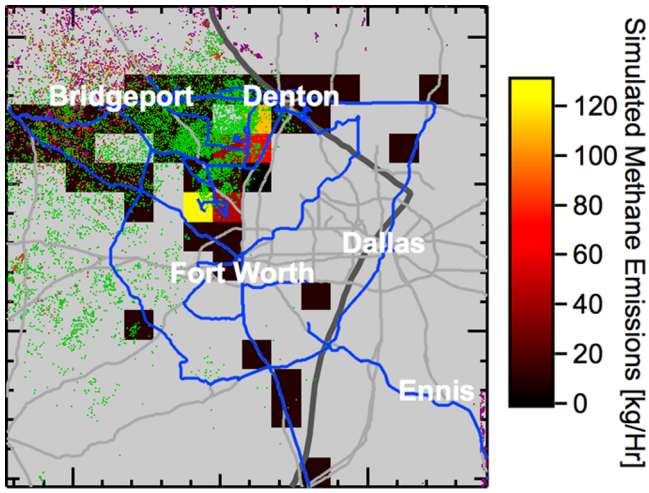

Figure 2. Map of simulated average methane emission magnitudes in and around the Barnett region. The region studied here spans 160 km^2, with a bin size of 10 km^2. A logarithmic color scale shows the average magnitude of emissions obtained via Gaussian plume simulation of all measurements within a given bin. Squares with no color indicate that no data was available. The blue lines trace the path followed by the mobile laboratories. The thick gray trace defines the eastern limit to the Barnett shale formation, with pale gray traces showing major roads and highways in the area. Locations[22] of oil, gas and mixed wells are shown as purple, green and orange dots, respectively.

emissions is concentrated in the area between Fort Worth and Denton. There are several landfills in this region, but only one was measured: a landfill southeast of Denton with emissions estimated at 23 kg/h (95% CI [8, 77] kg/h). The hot spots in the map in Figure 2 are thus largely dominated by oil and gas sources. For the data studied, lower average binned methane emissions were observed west of Bridgeport despite a high density of oil and gas producing wells. Some areas of the map in Figure 2 do not show any data even when a mobile laboratory

DOI: 10.1021/es506352j
Environ. Sci. Technol. 2015, 49, 7889−7895

transect was conducted nearby. The primary cause for this is periods of calm winds (wind speed <1 m/s), precluding a Gaussian plume analysis. Additional measurements, particularly in the area southwest of Fort Worth would enhance the spatial coverage of the current analysis.

The map in Figure 3 shows a coarse trend in ethane/methane enhancement ratio. Methane plumes with higher

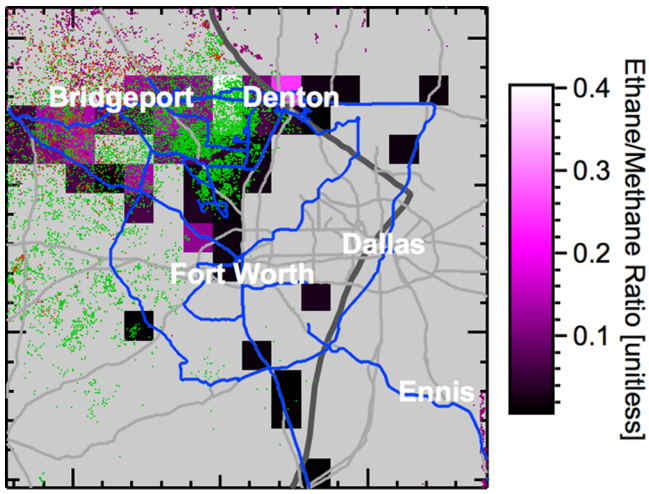

Figure 3. Map of measured ethane/methane enhancement ratios in and around the Barnett. A logarithmic color scale shows the average ethane/methane enhancement ratio for the same set of plumes shown in Figure 2 above. See Figure 2 caption for additional details.

ethane content were generally observed in the northwestern quadrant of the study area; lower ethane-content plumes were observed in areas to the south and east. This trend is consistent with the geographic distribution of oil production in the Barnett (see SI for plots of oil and gas production based on well production data[22]) and with the findings of other Barnett Coordinated Campaign studies.[20,21] While gas production spans a majority of the study area, oil production is concentrated in the north and west areas of the Barnett region. These locations are shown as colored dots on the maps in Figure 2 and Figure 3. Our data and analysis do not show any correlation between the magnitude of methane emissions and the ethane/methane enhancement ratio.

Individual Facilities. Several individual natural gas facilities are further investigated by constraining the position of the simulated point source. Some of these facilities are chosen based on their proximity to the drive paths and their reported methane inventory numbers. In other cases such as a well pad in DISH, TX, high emitters are identified via the *iterative forward dispersion* method and the locations of the simulation fine-tuned manually. The majority of the facilities chosen for this type of analysis are high-emitting and they should thus not be considered a representative sampling of all operations in the Barnett Shale.

In these analyses, satellite photographs and experimenter familiarity with natural gas equipment play an important role in determining the potential source locations. Updated map imagery was available for all cases analyzed, but may be a limitation in other study areas with active exploration, recent expansion and rapid changes in landscape. In cases where the observed plume shows clear structure, such as a processing plant near Bridgeport, individual pieces of equipment are chosen as the main source location (*multisource fixed release position* method). In other cases, the measurement is performed far enough downwind, several times further than the facility size, to broaden and mix any such distinctions. For these facilities, the source location is fixed (*fixed release position* method), and the experimental wind bearing replaced in the model with the bearing corresponding to the vector between measurement and facility location. Fixing the wind bearing is equivalent to allowing some flexibility in the exact simulated plume location, with the implicit assumption that the true facility location is known to a higher degree of certainty than the true wind bearing. The fixed wind bearings are within ~20° of the measured bearing (see SI for examples).

A plume from a natural gas compressor station near Eagle Mountain is shown in Figure 4. The location of the suspected

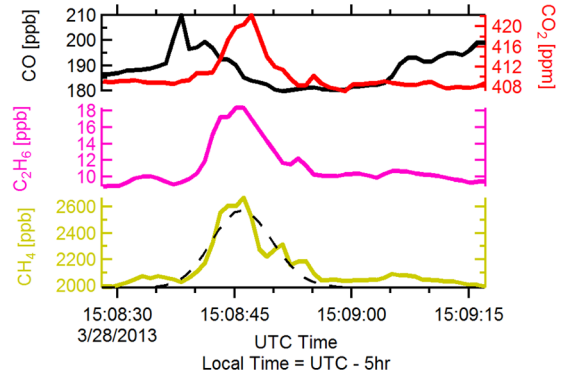

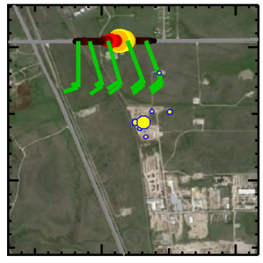

X [m]	Y [m]	kg/hr
18.7	-105.5	0
-25.1	-44.8	0
-58.6	0.8	10.8
0.0	0.0	43.2
64.4	83.0	0
196.4	80.5	3.6
119.9	370.8	0

Figure 4. Measured mixing ratios for carbon dioxide (red), carbon monoxide (black), ethane (magenta) and methane (gold) mixing ratios downwind of a natural gas compressor station near Eagle Mountain, TX. Results of the *multisource fixed release location* simulation (dotted black trace) overlay the observed methane mixing ratio. A map shows the segment of data in question with color getting warmer (from black to yellow) with increasing methane mixing ratio. Wind barbs pointing into the wind show the measured bearing and magnitude along the transect. The yellow markers on the map show the individual point sources chosen for this simulation. The table shows the individual offset distances (in meters) from the central chosen point source along with the simulated emissions in kg/h.

equipment is in the northern-most portion of the complex, indicated by the yellow dots. Though several potential sources were chosen for this site, including compressor houses and condensate storage tanks, the plume can be adequately simulated using only a subset of these sources. The presence of coemitted species helps in the choice of emission points. For example, in Figure 4, the presence of CO_2 and the ratios of CH_4/CO_2 and C_2H_6/CH_4 suggest a fugitive leak at a dry gas compressor (Roscioli et al.[23] describe many other source signatures); uncorrelated CO suggests the presence of other less efficient combustion sources such as generators or vehicles. In simulations of different plume intercepts of the same facility,

DOI: 10.1021/es506352j
Environ. Sci. Technol. 2015, 49, 7889−7895

the process is reinitialized, varying individual point source emissions to achieve good fit with experimental results. This allows for a better understanding of the variability in simulated emissions based on choice of sources. Averaging the simulated results of 4 replicate simulations of this facility's downwind plume (see SI) yields a final emission estimate of 51 kg/h (95% CI: [17, 170] kg/h). Emissions from the 2013 EPA GHGRP are 18.9 kg/h,[24,25] falling within the lower bound of the simulation's confidence interval; 2012 GHGRP emissions of 44.6 kg/h are somewhat closer.[4] A processing plant near Bridgeport, with emissions estimated here at 193 kg/h (95% CI: [64, 645] kg/h) also compares favorably to reported 2013 GHGRP emissions of 115 kg/h. This point source in addition to many others is discussed in detail by Lavoie et al.[26] and compared to measurements performed by other study collaborators using different methodologies.

Table 1 below lists additional individual sources with fixed locations. The facility latitude and longitude are outlined along with the simulated emission magnitude and the number of replicate plumes acquired, if any. Individual plume images similar to Figure 4 are shown in the SI. For some of the facilities in Table 1 and in the data set shown in Figure 1, there is uncertainty in the source attribution (location) in addition to the source magnitude due to the potential of other nearby sources. At far plume intercept distances, point sources within a large geographic area can each generate a simulated plume with good agreement with experiment. For other facilities, there is no question of the emission source due to replicate measurements, a lack of other possible sources, or visual identification of the facility when driving on a nearby public road. Those facilities with highly certain attribution are noted with an asterisk in Table 1. All uncertainties reported correspond to the 95% CI method error based on the staged tracer release data set.

Most of the sources highlighted in Table 1 consist of large natural gas facilities visited by study design, typically gas processing plants and compressor stations, supplemented with other accidental measurements of extreme emissions from smaller facilities like the well pads near Boyd, Justin, DISH, and others. Here, it is important to distinguish between the larger emissions expected from larger facilities versus extreme emissions from smaller operation sites. Extreme emitter well pad emission estimates from these results are used by Lyon et al. to supplement more representative distributions of well pad emissions for the Barnett inventory of emissions from natural gas operations[25] (see SI for well pad data set). Results from recent and ongoing studies[27,28] of the natural gas production,[19] transmission,[29] and gathering and processing[23,30] sectors of the oil and gas industry can be leveraged, and suggest that among the processing plants, gathering and compressor stations all but the gathering station near Cleburne are generally within the expected quantified emissions magnitudes for these sectors. In this data set, however, the gathering station near Cleburne is an exception and inspection of satellite maps do not reveal alternative or intervening sources.

The above results demonstrate how mobile and fast response measurements of methane and ethane, supplemented by other measurements (position, wind and other chemical tracers like CO_2), can be used to understand emissions at the individual facility level as well as the regional level. The accuracy of the Gaussian dispersion flux quantification used here is investigated: emission rates are quantified for staged tracer release data (with known emission rates) and results support a 95% CI of a factor of 0.334 on the lower side and a factor of 3.34 on the higher side.

Emissions for all measured methane plumes attributed to oil and gas operations in the Barnett shale region show an exponential distribution, supporting the use of a distribution of emission factors rather than an average emission factor in inventory calculations.[25,30,29] 19% of emitters have simulated methane emissions larger than 10 kg/h. For 2012 Texas gas prices of $2.66 per thousand cubic feet,[31] 98% methane content in natural gas, and assuming a sustained emission, this corresponds only to $12 K in lost revenue per year. The largest simulated emission of 1360 kg/h corresponds to over $1.2 million/year. Barring the presence of other regulatory tools like a carbon tax, the impact of such losses and thus the economic incentive to fix them will depend greatly on the size of the facility. The leak fraction,[30] or proportional loss,[32] translates to a fraction of revenue lost. In fact, additional analysis of selected facilities show that emissions vary broadly by source type, as is expected based on the typical size/capacity of these facilities (gas processing plant vs well pad for example). We have identified several large well pad emitters which are used in a related study quantifying the impact of production site superemitters, as defined by their proportional loss rates.[32] Our analysis shows enhanced average methane emission magnitudes in the central northern part of the study area (between Bridgeport, Fort-Worth and Denton).

Ethane content relative to methane is shown to be concentrated in the northwest portion of the study area, corresponding to areas with increased oil production. The distribution of ethane/methane ratios observed during these ground measurements is consistent with those values observed by aircraft,[21] with discrepancies attributed to differing sampling regions.

Despite the stringent meteorological and plume interception requirements and the model uncertainties involved, plume transect sampling and *iterative forward dispersion* simulations are useful tools for emissions investigation, allowing large areas to be covered in a short amount of time (here, nine plumes per hour of measurement are successfully quantified) without the need for facility access.

■ ASSOCIATED CONTENT

Supporting Information

Description and error quantification for the dispersion method used, data set filtering, binned natural gas and oil production maps, and individual dispersion results for selected plumes. This material is available free of charge via the Internet at http://pubs.acs.org.

■ AUTHOR INFORMATION

Corresponding Author

*Phone: (978) 663-9500, ×228; e-mail: tyacovitch@aerodyne.com.

Notes

The authors declare no competing financial interest.

■ ACKNOWLEDGMENTS

This work was supported by the Environmental Defense Fund's Methane Study. We acknowledge the support of Shell Global Solutions, Project 4550081333, in the generation of the dataset used in dispersion model development and uncertainty analysis.

DOI: 10.1021/es506352j
Environ. Sci. Technol. 2015, 49, 7889−7895

REFERENCES

(1) Alvarez, R. A. Using multi-scale measurements to improve methane emissions estimates from oil and gas operations in the Barnett shale, Texas: Campaign summary. *Curr. Opin. Chem. Eng.* **2014**, submitted.

(2) Herndon, S. C.; Jayne, J. T.; Zahniser, M. S.; Worsnop, D. R.; Knighton, B.; Alwine, E.; Lamb, B. K.; Zavala, M.; Nelson, D. D.; McManus, J. B.; et al. Characterization of urban pollutant emission fluxes and ambient concentration distributions using a mobile laboratory with rapid response instrumentation. *Faraday Discuss.* **2005**, *130*, 327 DOI: 10.1039/b500411j.

(3) Pétron, G.; Frost, G.; Miller, B. R.; Hirsch, A. I.; Montzka, S. A.; Karion, A.; Trainer, M.; Sweeney, C.; Andrews, A. E.; Miller, L.; et al. Hydrocarbon emissions characterization in the Colorado Front Range: A pilot study. *J. Geophys. Res.: Atmos.* **2012**, *117* (D4), D04304 DOI: 10.1029/2011JD016360.

(4) United States Environmental Protection Agency. Greenhouse gas reporting program, 2012. http://ghgdata.epa.gov/ghgp/main.do.

(5) Kolb, C. E.; Herndon, S. C.; McManus, J. B.; Shorter, J. H.; Zahniser, M. S.; Nelson, D. D.; Jayne, J. T.; Canagaratna, M. R.; Worsnop, D. R. Mobile laboratory with rapid response instruments for real-time measurements of urban and regional trace gas and particulate distributions and emission source characteristics. *Environ. Sci. Technol.* **2004**, *38*, 5694.

(6) Nelson, D. D.; McManus, B.; Urbanski, S.; Herndon, S.; Zahniser, M. S. High precision measurements of atmospheric nitrous oxide and methane using thermoelectrically cooled mid-infrared quantum cascade lasers and detectors. *Spectrochim. Acta, Part A* **2004**, *60* (14), 3325.

(7) Yacovitch, T. I.; Herndon, S. C.; Roscioli, J. R.; Floerchinger, C.; McGovern, R. M.; Agnese, M.; Pétron, G.; Kofler, J.; Sweeney, C.; Karion, A.; et al. Demonstration of an ethane spectrometer for methane source identification. *Environ. Sci. Technol.* **2014**, *48* (14), 8028 DOI: 10.1021/es501475q.

(8) Crosson, E. R. A cavity ring-down analyzer for measuring atmospheric levels of methane, carbon dioxide, and water vapor. *Appl. Phys. B: Laser Opt.* **2008**, *92* (3), 403 DOI: 10.1007/s00340-008-3135-y.

(9) Weather Underground, 2014. Archival wind and weather data. http://www.wunderground.com (accessed October, 2014).

(10) Beychok, M. R. *Fundamentals of Stack Gas Dispersion*; 4th ed.; published by author: Irvine, CA, 2005.

(11) United States Environmental Protection Agency. STAR (STability ARray program), 2014. http://www.epa.gov/ttn/scram/metobsdata_procaccprogs.htm#star (accessed August 28, 2014).

(12) Thoma, E. D.; Squier, B. C.; Olson, D.; Gehrke, G.; Eisele, A. P.; Miller, M.; DeWees, J. M.; Segall, R. R.; Amin, M. S.; Modrak, M. T. Assessment of methane and VOC emissions from select oil and gas production operations using remote measurements, interim report on survey studies in CO, TX and WY. In AWMA Symposium on Air Quality Measurement Methods and Technology, Durham, North Carolina, 2012.

(13) Brantley, H. L.; Thoma, E. D.; Squier, W. C.; Guven, B. B.; Lyon, D. Assessment of methane emissions from oil and gas production pads using mobile measurements. *Environ. Sci. Technol.* **2014**, *48* (24), 14508 DOI: 10.1021/es503070q.

(14) Fritz, B. K.; Shaw, B. W.; Parnell, C. B. J. Influence of meteorological time frame and variation on horizontal dispersion coefficients in gaussian dispersion modeling. *Trans. ASABE* **2005**, *48* (3), 1185 DOI: 10.13031/2013.18501.

(15) Abdel-Rahman, A. A. On the dispersion models and atmospheric dispersion. In *2nd International Conference on Waste Management, Water Pollution, Air Pollution, Indoor Climate*, Corfu, Greece, October 26−28, 2008; Mastorakis, N. E., Ed.; WSEAS Press; Athens, Greece, 2008; pp 31−39, ISBN: 978-960-474-017-8.

(16) Beychok, M. R. Error propagation in air dispersion models, 2014. http://www.air-dispersion.com/feature.html (accessed August 28, 2014).

(17) Sax, T.; Isakov, V. A case study for asessing uncertainty in local-scale regulatory air quality modeling applications. *Atmos. Environ.* **2003**, *37*, 3481 DOI: 10.1016/S1352-2310(03)00411-4.

(18) Lamb, B. K.; McManus, J. B.; Shorter, J. H.; Kolb, C. E.; Mosher, B.; Harriss, R. C.; Allwine, E.; Blaha, D.; Howard, T.; Guenther, A.; et al. Development of atmospheric tracer methods to measure methane emissions from natural-gas facilities and urban areas. *Environ. Sci. Technol.* **1995**, *29* (6), 1468.

(19) Allen, D. T.; Torres, V. M.; Thomas, J.; Sullivan, D. W.; Harrison, M.; Hendler, A.; Herndon, S. C.; Kolb, C. E.; Fraser, M. P.; Hill, A. D.; et al. Measurements of methane emissions at natural gas production sites in the United States. *Proc. Natl. Acad. Sci. U. S. A.* **2013**, *110* (44), 17768 DOI: 10.1073/pnas.1304880110.

(20) Karion, A.; Sweeney, C.; Kort, E. A.; Shepson, P.; Conley, S.; Wolter, S.; Smith, M. L.; Petron, G.; Lavoie, T.; Cambaliza, M. Aircraft-based estimate of total methane emissions from the Barnett shale region. *Environ. Sci. Technol.* **2014**, submitted.

(21) Smith, M. L.; Kort, E. A.; Karion, A.; Sweeney, C.; Herndon, S. C.; Newberger, T.; Wolter, S.; Yacovitch, T. I. Airborne ethane observations in the Barnett shale: Quantification of ethane flux and attribution of methane emissions. *Environ. Sci. Technol.* **2014**, submitted.

(22) *DI Desktop*; Drillinginfo—An International Oil & Gas Intelligence Company: Austin, TX, 2013.

(23) Roscioli, J. R.; Yacovitch, T. I.; Floerchinger, C.; Mitchell, A. L.; Tkacik, D. S.; Subramanian, R.; Martinez, D. M.; Vaughn, T. L.; Williams, L.; Zimmerle, D.; et al. Measurements of methane emissions from natural gas gathering facilities and processing plants: Measurment methods. *Atmos. Meas. Technol. Discuss.* **2015**, *7*, 12357 DOI: 10.5194/amtd-7-12357-2014.

(24) United States Environmental Protection Agency. Greenhouse gas reporting program, 2013. http://ghgdata.epa.gov/ghgp/main.do.

(25) Lyon, D. Constructing a spatially-resolved methane emission inventory for the Barnett shale region. *Environ. Sci. Technol.* **2014**, submitted.

(26) Lavoie, T. N.; Shepson, P. B.; Cambaliza, M. O.; Karion, A.; Sweeney, C.; Kort, E.; Hirst, B.; Yacovitch, T. I.; Herndon, S. C.; Lan, X. Aircraft-based measurements of point source methane emissions in the Barnett shale basin. *Environ. Sci. Technol.* **2014**, submitted.

(27) Gathering facts to find climate solutions, 2014. Environmental Defense Fund Website. http://www.edf.org/climate/methane-studies (accessed January 31, 2014).

(28) What will it take to get sustained benefits from natural gas?, 2013. Environmental Defense Fund Website. http://www.edf.org/methaneleakage (accessed November 12, 2013).

(29) Subramanian, R.; Williams, L. L.; Vaughn, T. L.; Zimmerle, D.; Roscioli, J. R.; Herndon, S. C.; Yacovitch, T. I.; Floerchinger, C.; Tkacik, D. S.; Mitchell, A. L.; et al. Methane emissions from natural gas compressor stations in the transmission and storage sector: Measurements and comparisons with the epa greenhouse gas reporting program protocol. *Environ. Sci. Technol.* **2015**, DOI: 10.1021/es5060258.

(30) Mitchell, A. L.; Tkacik, D. S.; Roscioli, J. R.; Herndon, S. C.; Yacovitch, T. I.; Martinez, D. M.; Vaughn, T. L.; Williams, L. L.; Sullivan, M. R.; Floerchinger, C.; et al. Measurements of methane emissions from natural gas gathering facilities and processing plants: Measurement results. *Environ. Sci. Technol.* **2015**, DOI: 10.1021/es5052809.

(31) *U.S. Natural Gas Wellhead Price*; U.S. Energy Information Administration; U.S. Department of Energy; Washington, DC, 2015. http://www.eia.gov/dnav/ng/hist/n9190us3a.htm (accessed February 19, 2015).

(32) Zavala-Araiza, D.; Lyon, D.; Alvarez, R. A.; Hamburg, S. P.Towards a functional definition of methane super-emitters: Application to natural gas production sites. *Environ. Sci. Technol.* **2014**, submitted

DOI: 10.1021/es506352j
Environ. Sci. Technol. 2015, 49, 7889−7895